Environ Earth Sci (2017) 76:569
DOI 10.1007/s12665-017-6909-x

ORIGINAL ARTICLE

Drought analysis in New Zealand using the standardized precipitation index

Tommaso Caloiero[1]

Received: 16 February 2017 / Accepted: 14 August 2017 / Published online: 21 August 2017

Abstract The present article investigates drought events in New Zealand through the application of the SPI at various timescales (3, 6, 12 and 24 months). First, a temporal analysis has been performed, and the most severe dry episodes have been detected. Then, the spatial distribution of the percentage of data falling within the different level of drought has been evaluated. In addition, a trend analysis has been conducted at seasonal scale, considering the wet and the dry seasons, and at annual scale. Finally, the relationship between drought and ENSO has been investigated. Results show that, in every area currently subject to drought, an increase in this phenomenon can be expected. Specifically, the results of this paper highlight that agricultural regions on the Eastern side, such as the Canterbury Plains, are the most consistently vulnerable areas, as well as other regions in the North Island, including primary industry regions like Waikato. Moreover, a clear link between drought and the two phases of the ENSO has been detected.

Keywords Drought · SPI · Trend · New Zealand

Introduction

In the last decade, climate change and its negative impacts on ecosystems, agriculture, water supply and management, human welfare and regional political stability drew considerable international attention due to the increase of phenomena such as flood, heat waves, forest fires and droughts (Estrela and Vargas 2012). In this context, research on regional and local scale changing patterns of precipitation is paramount for the assessment of hydrological extremes (Huang et al. 2015). For example, following precipitation and/or evapotranspiration variability which, recently, have been evidenced worldwide (IPCC 2013), drought is expected to become more frequent in the twenty-first century in some seasons and areas.

Meteorological drought consists of temporary lower-than-average precipitation and results in diminished water resources availability and carrying capacity of the ecosystems (Tabari et al. 2012) which impact on economic activities, human lives and the environment (Bayissa et al. 2015). In recent years, several researchers have analysed drought events in several parts of the world (e.g. Bordi et al. 2009; Minetti et al. 2010; Feng et al. 2011; Hannaford et al. 2011; Fang et al. 2013; Hua et al. 2013; Buttafuoco and Caloiero 2014; Sirangelo et al. 2015, 2017), even though drought phenomena are difficult to detect and monitor due to their complex nature. Usually, drought severity is evaluated by means of drought indices (Wilhite et al. 2000; Tsakiris et al. 2007). Among these indices, the standardized precipitation index (SPI; McKee et al. 1993, 1995) has found widespread application worldwide because it can be evaluated for different timescales and allows the analysis of different drought categories. For this reasons, the SPI is considered to be one of the most robust and effective drought indices (Capra and Scicolone 2012). Moreover, the evaluation of the SPI requires only precipitation data, making it easier to calculate than more complex indices, and allows the comparison of drought conditions in different regions and for different time

✉ Tommaso Caloiero
tommaso.caloiero@isafom.cnr.it

[1] National Research Council (CNR), Institute for Agricultural and Forest Systems in the Mediterranean (ISAFOM), Via Cavour 4/6, 87036 Rende, CS, Italy

periods (Wu et al. 2005; Vicente-Serrano 2006; Buttafuoco et al. 2015; Caloiero et al. 2016).

Since agriculture is one of the largest sectors of the tradable economy, a period of drought in New Zealand can have significant ecological, social and economic impacts (Palmer et al. 2015). In fact, New Zealand experiences rainfall deficits and short duration of dry spells which are not as unusual as isolated drought events at regional level. For example, the widespread drought event which affected New Zealand from late 2007 to the end of autumn 2008, caused damages of about 2.8 billion of New Zealand dollars (MAF 2009). The 2013 drought in New Zealand was estimated to have caused the Gross Domestic Product (GDP) to fall by 0.6% (Kamber et al. 2013). Regional scenarios of drought in New Zealand evidenced an increase in drought trend during this century in all the areas that are presently subject to drought (Mullan et al. 2005). Furthermore, based on the latest climate and impact modelling, more droughts could be expected in the future in some locations such as the agricultural regions on the Eastern coast and, particularly, the Canterbury Plains, as well as Northland (Clark et al. 2011).

In this study, drought events in New Zealand have been evaluated using the SPI at various timescales (3, 6, 12 and 24 months). This study aims to identify the most severe drought events which affected New Zealand, to analyse the evolution of the drought episodes through the identification of the SPI trend at different timescales in the period 1951–2012 and to investigate the possible relationship between drought and the El Niño-Southern Oscillation (ENSO).

Study area and data

New Zealand is located at 34°10′50″ to 46°55′50″S in the Southern Hemisphere, 2500 km east of the Australian continent. Its two islands have a rather elongated shape, 1930 km from north to south, and a maximum width of 400 km, comprising a total surface of about 270,000 km^2. Mountain ranges reach an altitude of 3724 m (Fig. 1). New Zealand weather reflects the one of other similar locations in those latitudes (Garnier 1950; Dravitzki and McGregor 2011). Its climatic conditions are mainly influenced by some physical factors (Oliver 2005). Firstly, the oceans surrounding New Zealand affect air circulation and seasonal climate. Air masses from the tropical zones of the Pacific cause the weather to be considerably humid and with temperatures ranging between 18 and 21 °C. Instead, oceanic currents from Antarctica are responsible for colder temperatures between 7 and 13 °C and high rainfall amounts. Consequently, New Zealand generally presents cool summers and mild winters; however, cold air from Antarctica is also responsible for occasional snow and frost. Therefore, the presence of the ocean results in fresh summers and mild winters, although snow and frost are likely to occur as a consequence of cold air coming from Antarctica.

The mountains crossing both the North Island and the South Island to the west is the second factor impacting on air circulation and determining New Zealand climate (Griffiths 2011; Jiang et al. 2013). The 750-km-long, over 3000-m-high Southern Alps traversing the South Island constitute a barrier against air flows coming in from the south–south-west direction (Tomlinson 1976). Specifically, they block the air that would flow upstream, producing lee troughs on the downwind side as a consequence of their dynamic uplift and vertical mixing on the upwind edge. Considerable differences in the rainfall amounts can occur over the short distance between the windward mountain slopes and the rain shadows a few kilometres eastward.

Finally, the nearby Australian continental landmass influences New Zealand's seasonal climate, since the former's eastern land/sea boundary presents a cyclogenesis region which moves towards the Tasman sea (Trenberth 1991; Sinclair 1994, 1995a, b). Very large spatial differences in precipitation can occur over the short distance (Trenberth 1991; Sinclair 1994, 1995a, b). Clear sky in winter leads to considerable surface cooling which, in turn, results in stable lower atmospheric conditions. By contrast, in the summer, large convective hot air masses coming from Australia cause robust airflows which persistently affect New Zealand (Oliver 2005).

A thorough analysis of New Zealand's climate on both islands had been carried out, and its results were published by The National Institute of Water and Atmosphere Research (NIWA) of New Zealand (NIWA 2013). According to NIWA, the North Island is a subtropical area characterised by warm humid summers and mild winters. Winter presents the highest degree of climatic instability and is the rainiest period of the year. Tropical storms occur in summer and autumn with high winds and severe precipitation. Stable, dry and warm summers are typical of the Central region of the North Island, whereas unstable cool winters occur. In the south-western part of the North Island, weather is generally more stable in summer and at the beginning of autumn; summers are usually warm, while winters are not very cold. The eastern North Island area presents a dry, sunny climate and warm dry settled summer weather. Heavy rainfall can occur from the east or the south-east (NIWA 2013). As regards the South Island, its northern part is the sunniest region in New Zealand with summers characterised by warm dry and stable weather. Although extreme yearly precipitation is considerably higher than average, the Western South Island area may experience occasional dry spells towards the end of the

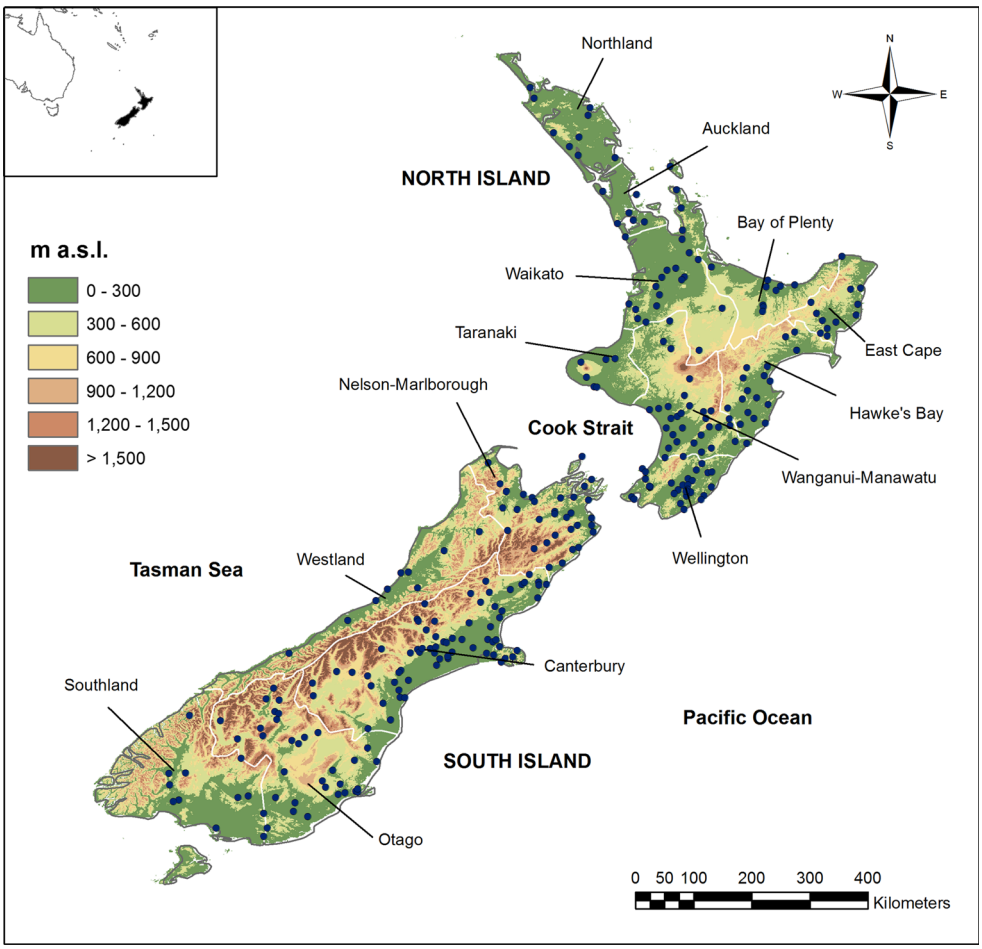

Fig. 1 Location of the selected 294 rain gauge stations on a DEM of New Zealand

summer and in the winter months, while intense precipitation from the north-west is present. The climate of the Eastern and Inland areas of the South Island is influenced by the Southern Alps. In particular, long periods of dryness characterise the summer season in this area, which also presents low mean annual rainfall. Overall, the majority of the Southern New Zealand area is traversed by unsettled weather coming from the south and south-west across the sea and experiences cool coastal breezes (NIWA 2013).

In order to carry out a SPI analysis at different timescales, the New Zealand National Climate database of the National Institute of Water and Atmospheric Research (NIWA) has been selected. Several studies on New Zealand's climate (Salinger and Mullan 1999; Griffiths et al. 2003; Dravitzki and McGregor 2011; Caloiero 2014, 2017) made extensive use of this database, which presents high-quality data and complete, or near-complete, records for the period 1951–2012. Until 2012, the New Zealand National Climate database consisted of measurements collected at 3011 stations, with a density of 1 station per 89 km^2. In particular, for the present analysis, the monthly rainfall data were extracted and used, after performing record error checks and metadata analyses for inhomogeneities detection. Following these procedures, a number of station series, which presented either low-quality records or too low a number of years of observation for statistical purposes (<50 available years of data), were discarded. The series ending before 2010 and those showing more than 5% of data lacking were also discarded. Thus, the final selection included 294 series longer than 50 years with a density of 1 station per 913 km^2 (Fig. 1).

Methodology

In this study, dry and wet periods were evaluated using the SPI at different timescale (3, 6, 12 and 24 months). In fact, while the 3- and 6-month SPI describe droughts that affect plant life and farming, the 12- and 24-month SPI influence the way water supply/reserves are managed (Edwards and McKee 1997; Bonaccorso et al. 2003). Angelidis et al. (2012) offered a meticulous description of the method to compute the SPI.

In order to compute the index, for each timescale and for each location in space, an appropriate probability density function (PDF) must be fitted to the frequency distribution

of the cumulated precipitation. In particular, a gamma function is considered. The shape and the scale parameters must be estimated for each month of the year and for each time aggregation, for example by using the approximation of Thom (1958).

Since the gamma distribution is undefined for a rainfall amount $x = 0$, in order to take into account the zero values that occur in a sample set, a modified CDF must be considered:

$$H(x) = q + (1 - q)\, G(x) \tag{1}$$

with $G(x)$ the cumulative distribution function (CDF), q the probability of zero precipitation, given by the ratio between the number of zero in the rainfall series (m) and the number of observations (n).

Finally, the CDF is changed into the standard normal distribution by using, for example, the approximate conversion provided by Abramowitz and Stegun (1965):

$$z = \mathrm{SPI} = -\left(t - \frac{c_0 + c_1 t + c_2 t^2}{1 + d_1 t + d_2 t^2 + d_3 t^3}\right), \quad t = \sqrt{\ln\left(\frac{1}{(H(x))^2}\right)} \quad \text{for } 0 < H(x) < 0.5 \tag{2}$$

$$z = \mathrm{SPI} = +\left(t - \frac{c_0 + c_1 t + c_2 t^2}{1 + d_1 t + d_2 t^2 + d_3 t^3}\right), \quad t = \sqrt{\ln\left(\frac{1}{(1 - H(x))^2}\right)} \quad \text{for } 0.5 < H(x) < 1 \tag{3}$$

with c_0, c_1, c_2, d_1, d_2 and d_3 mathematical constants.

Table 1 reports the climatic classification according to the SPI, provided by the National Drought Mitigation Center. This index is now habitually used in the classification of wet periods, even though the original classification provided by McKee et al. (1993) was limited to drought periods only.

In order to evaluate the possible existence of temporal tendencies, the SPI series were analysed for trends with the well-known Mann–Kendall (MK) nonparametric test (Mann 1945; Kendall 1962). For specified significance levels α (90–95–99%), the statistical significance of the trend has been evaluated using a two-tailed test.

Finally, the connections between drought and large-scale atmospheric patterns were investigated by means of the Pearson's product-moment coefficient applied to the SPI values and the ENSO values in its phases (El Niño and La Niña). In particular, El Niño and La Niña years were identified using the Southern Oscillation Index (SOI), which is a standardised index based on the observed sea level pressure differences between Tahiti and Darwin (Vicente-Serrano 2005). In general, smoothed time series of the SOI correspond very well to changes in ocean temperatures across the eastern tropical Pacific. The negative phase of the SOI represents below-normal air pressure at Tahiti and above-normal air pressure at Darwin. Prolonged periods of negative (positive) SOI values coincide with abnormally warm (cold) ocean waters across the eastern tropical Pacific typical of El Niño (La Niña) episodes. The values of the climatic index used in the study were provided by NOAA's National Centers for Environmental Information (NCEI). The statistical significance (95%) of the regression was checked by using the two-tailed test of the Student's t-distribution by evaluating the probability of rejecting the null hypothesis regarding the absence of any relationship for the values of t with (N-2) degrees of freedom.

Table 1 Climate classification according to the SPI values

SPI value	Class	Probability (%)
SPI $\geq$ 2.0	Extremely wet	2.3
1.5 $\leq$ SPI < 2.0	Severely wet	4.4
1.0 $\leq$ SPI < 1.5	Moderately wet	9.2
0.0 $\leq$ SPI < 1.0	Mildly wet	34.1
−1.0 $\leq$ SPI < 0.0	Mild drought	34.1
−1.5 $\leq$ SPI < −1.0	Moderate drought	9.2
−2.0 $\leq$ SPI < −1.5	Severe drought	4.4
SPI < −2.0	Extreme drought	2.3

Results and discussion

The analysis allowed the computation of the SPI at various temporal scales and subsequently the identification of numerous dry episodes for the 294 rain gauges. Figure 2 shows the temporal distribution, for the period 1951–2012, of the percentage of rain gauges that can be classified as Severe or Extreme Dry conditions (SED: SPI < −1.5) and allows to immediately detect the worst dry events. As regards the 3- and 6-month SPI, the twentieth century has been characterised by numerous dry periods. One of the first drought events took place in 1958 with more than 40 and 60% of the rain gauges showing SED, respectively, for the 3-month and the 6-month timescales. Within the 3- and 6-month intervals, another significant occurrence dates back to 1969, with about 45% (3 month) and 50% (6 month) of the rain gauges presenting SED. Dry conditions were also present in the year 1973 for both the 3- and the 6-month SPI with 40% plus rain gauges affected by SED. In the twenty-first century, the worst drought events have been detected in 2001, in particular for the 3-month SPI with almost 60% of the rain gauges presenting SED,

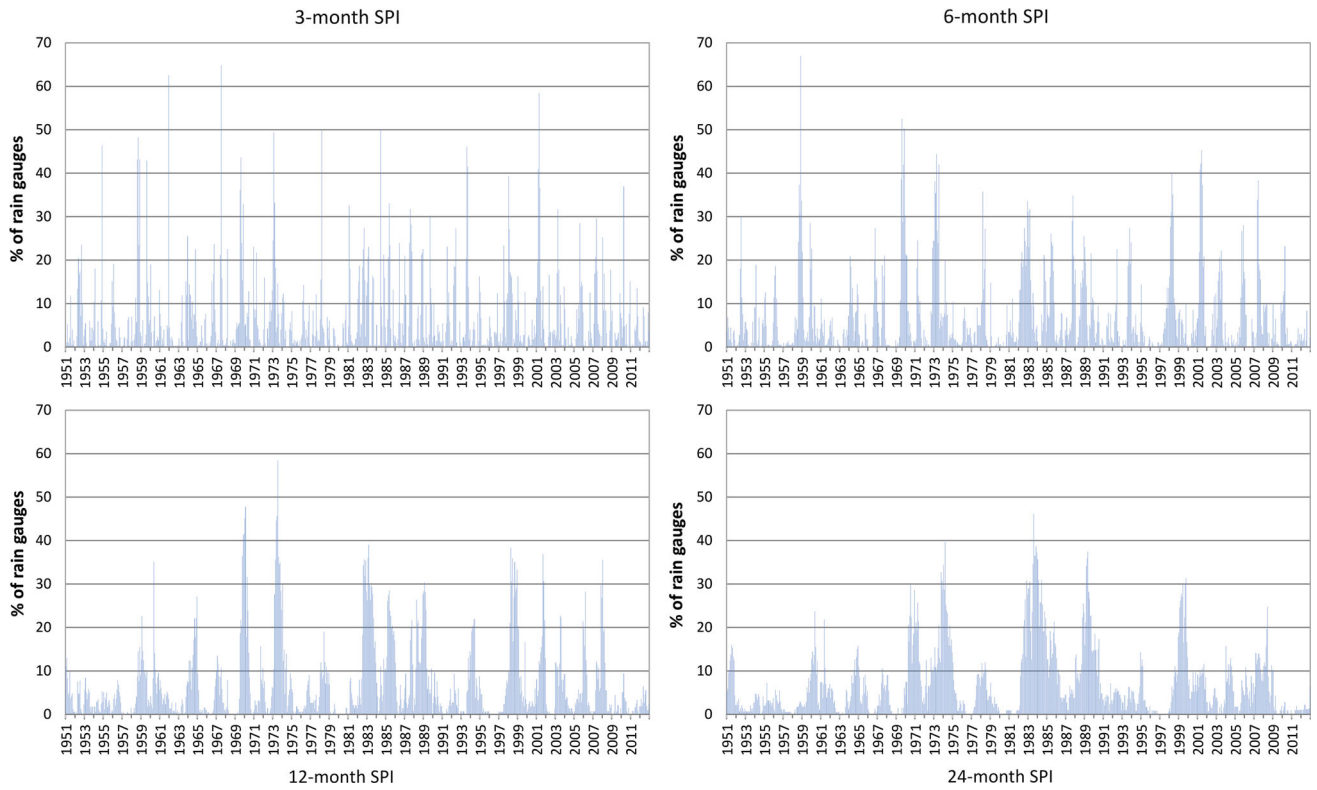

Fig. 2 Temporal distribution of the percentage of rain gauges which fell within severe or extreme dry conditions (SPI < -1.5)

and in 2007, for the 6-month SPI with almost 40% of the rain gauges presenting SED.

The 12- and 24-month SPI (Fig. 2) and the 3- and 6-month SPI clearly behave in a different way. Specifically, the main drought events, for both the 12-month and the 24-month timescales, occurred after 1970. Only in 1969, significant SPI values have been evaluated, with SED involving about 40% of the rain gauges. Since the 1970s, various drought episodes were registered, such as the extremely severe and prolonged drought event detected between 1982 and 1984. During this time, the 12-month SPI evidences 13 straight months of SED with about 40% of the rain gauges. As to what concerns the SPI over a 24-month period, 18 consecutive months present SED in an area ranging from 20% to almost 45% of the rain gauges, for the same time period. Remarkable events have been also observed in 1973 and 1989 even though with a different behaviour. In fact, while the first is the most diffuse event for the 12-month SPI, with more than 60% of the rain gauges showing SED, the second event was particular relevant for the 24-month SPI with almost 40% of the rain gauges presenting SED.

In Fig. 3, the spatial distribution of the percentage of data falling within the different levels of drought is presented. While for the 3- and the 6-month SPI only few areas of New Zealand showed high percentage of drought data, the 12- and the 24-month SPI evidenced wide areas affected by drought. These areas are mainly located in the central-east side of both the Islands. As a result, drought in New Zealand seems to be more related with water resource management problems than with problems deriving from vegetation and agricultural practices.

In order to detect drought temporal evolution in the period 1951–2012, the 294 series were tested for trend through the Mann–Kendall test. In particular, the trend analysis has been conducted at seasonal scale (February/Summer, May/Autumn, August/Winter and November/Spring SPI-3), considering the wet and the dry seasons (February and August SPI-6) and at annual scale (December SPI-12 and SPI-24 series). At seasonal scale (Fig. 4), a negative SPI values trend occurred in summer and autumn, with more than 15% and about 40% of the rain gauges showing a negative trend (significant level SL = 90%) in summer and in autumn, respectively. Moreover, considering a SL = 95%, more than 20% of the rain gauges presented a negative trend of the SPI in autumn. By contrast, in winter and spring, a positive SPI trend, more marked in spring, has been detected, involving about 10% and about 20% of the rain gauges (SL = 90%). From a spatial point of view, in summer and autumn, a clear negative trend has been detected in the eastern side of both the Islands. In particular, as to what concerns the

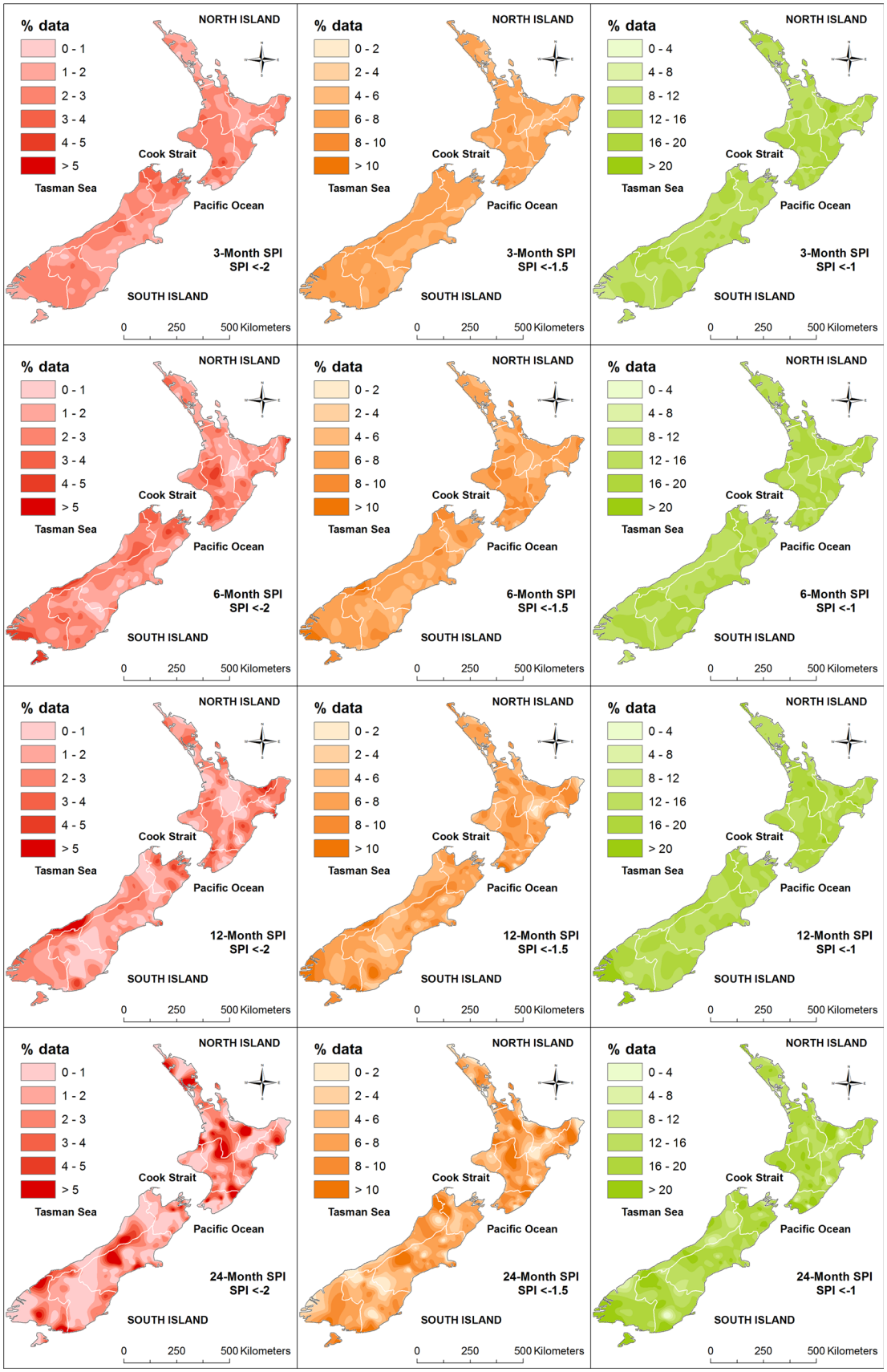
% data
0 - 1
1 - 2
2 - 3
3 - 4
4 - 5
> 5
0 - 2
2 - 4
4 - 6
6 - 8
8 - 10
> 10
0 - 4
4 - 8
8 - 12
12 - 16
16 - 20
> 20
NORTH ISLAND
SOUTH ISLAND
Cook Strait
Tasman Sea
Pacific Ocean
3-Month SPI SPI <-2
3-Month SPI SPI <-1.5
3-Month SPI SPI <-1
6-Month SPI SPI <-2
6-Month SPI SPI <-1.5
6-Month SPI SPI <-1
12-Month SPI SPI <-2
12-Month SPI SPI <-1.5
12-Month SPI SPI <-1
24-Month SPI SPI <-2
24-Month SPI SPI <-1.5
24-Month SPI SPI <-1
0 250 500 Kilometers

◀**Fig. 3** Spatial distribution of the percentage of monthly data falling within the different level of drought

summer period, the negative trend mainly involved the Canterbury, and the Nelson–Marlborough areas, while a positive trend has been identified in the Otago and the Westland areas (Fig. 4).

The marked SPI trend evaluated in spring and autumn highly impacts on the 6-month SPI trend detected in the dry and in the wet season (Fig. 5). In fact, the dry season (February SPI-6) showed similar percentage values of positive and negative trend, while in the wet season a predominant negative trend can be observed. Specifically, in the dry season, almost 15% of the rain gauges presented a positive trend (significant level SL = 90%) while about 10% of the rain gauges showed a negative trend. Conversely, in the wet period, more than 22% and about 14% of the rain gauges showed a negative trend with SL = 90% and SL = 95%, respectively. The negative trends detected

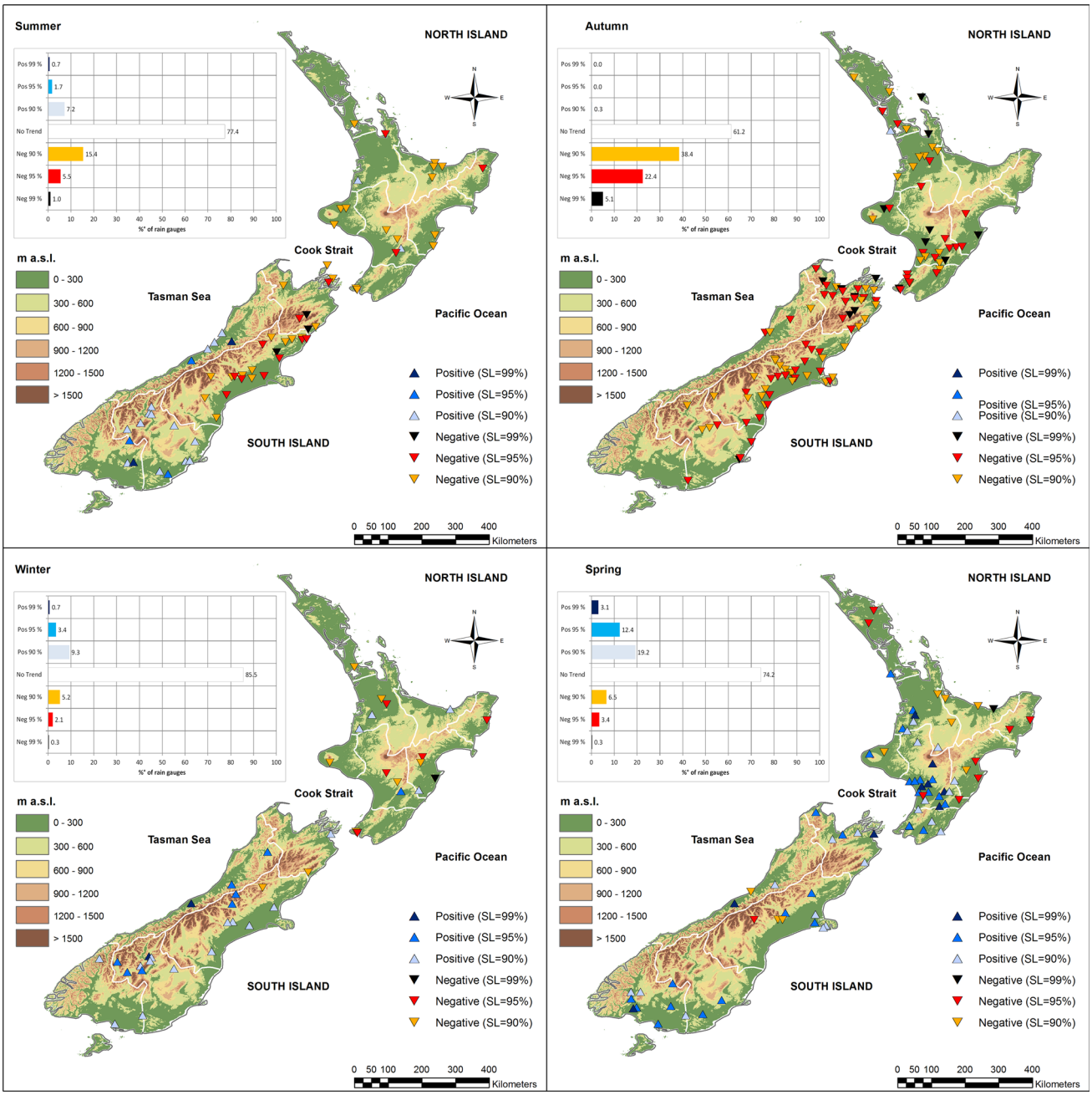

Fig. 4 Spatial distribution of the rain gauges presenting positive or negative rainfall trends (seasonal scale) and histogram with the trend results expressed as % of rain gauge of the whole data set

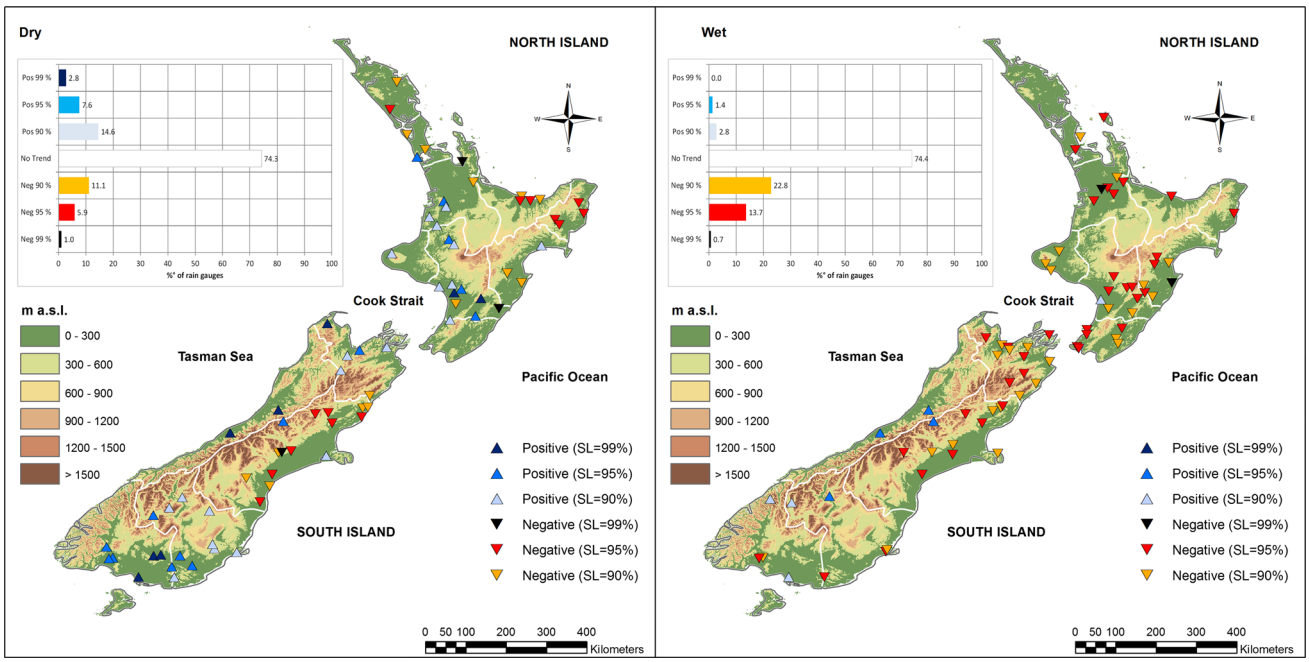

Fig. 5 Spatial distribution of the rain gauges presenting positive or negative rainfall trends (wet and the dry seasons) and histogram with the trend results expressed as % of rain gauges of the whole dataset

in the dry season are located in the Canterbury region, in the South Island, and in the East Cape and Bay of Plenty regions, in the North Island, while the positive trends have been mainly identified in the Otago, Southland and Nelson–Marlborough regions and in the south-western side of the North Island (Fig. 5).

Finally, at annual scale, a prevalent negative trend can be observed both for the 12-month and for the 24-month SPI (Fig. 6). In fact, as regards the 12-month SPI, 19% and more than 10% of the rain gauges showed a negative trend, respectively, for a SL = 90% and a SL = 95%. Similarly, for the 24-month SPI, more than 21% (significant level SL = 90%) and about 16% (significant level SL = 95%) of the rain gauges evidenced a negative trend. For both the 12-month and the 24-month SPI, the negative trend has been mainly detected in the Canterbury region and in the eastern side of the Nelson–Marlborough region, in the South Island, and in the Wanganui-Manawatu, East Cape, Hawke's Bay and Bay of Plenty regions, in the North Island. Instead, a positive trend has been evaluated in the Otago, Southland and Westland regions, in the South Island, and in the western side of the North Island (Fig. 6).

With the aim to assess the drought response to the global circulation variability, a correlation analysis between drought (at seasonal scale, considering the wet and the dry seasons and at annual scale) and El Niño (Fig. 7) and La Niña (Fig. 8) SOI phases was computed for each station. As a result, a clear link existing between drought and the two phases of the climatic index has been evidenced. In particular, El Niño impacts on drought especially during summer, autumn and in the dry season, in the eastern side of both islands (Fig. 7), while La Niña influences drought mainly along the coastal areas, and thus shows a lesser influence than El Niño (Fig. 8).

Current global level assessments suggest that droughts are expected to both increase and decrease following future climate change depending upon geographic location (Wang 2005). Based on the latest climate and impact modelling, New Zealand can expect more droughts in the future in some locations (Clark et al. 2011). As a result, this work has evidenced an increase in drought trend in all the areas that are presently subject to drought, supporting what has been evidenced in past studies (Mullan et al. 2005). In fact, the results of this paper confirm the geographic pattern of change found by Mullan et al. (2005), which mainly detected a drought increase in the future projections on the East Coast and no change in drought projections for the West Coast of the South Island. Specifically, as also evidenced by Clark et al. (2011), the results of this paper highlight that key agricultural regions on the Eastern side such as the Canterbury Plains are the most consistently vulnerable areas, together with other regions in the North Island, including key primary industry regions like Waikato. Furthermore, this paper confirmed past studies which evidenced that New Zealand's climate is influenced by modes of interannual and decadal-scale variability such as the ENSO. In fact, according to several authors (e.g. Salinger and Mullan 1999; Salinger et al. 1995; Griffiths et al.

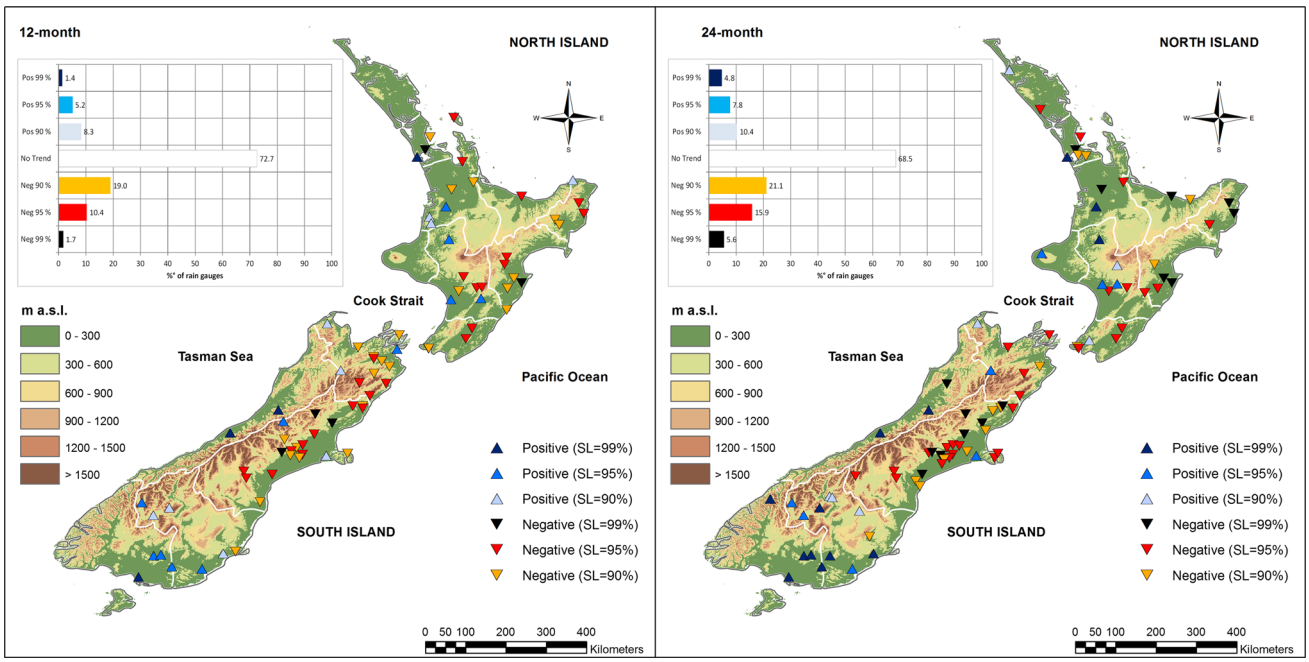

Fig. 6 Spatial distribution of the rain gauges presenting positive or negative rainfall trends (annual scale) and histogram with the trend results expressed as % of rain gauges of the whole dataset

2003; Griffiths 2007; Ackerley et al. 2012), negative phases of ENSO result in more frequent and stronger westerly and south-westerly winds over New Zealand, which lead to increased precipitation in the west and reduced precipitation in the east, whereas positive phases of ENSO result in increased northerly and easterly winds and decreased precipitation in the west.

Conclusion

In this study, drought events in New Zealand have been evaluated using the SPI at various timescales (3, 6, 12 and 24 months). First, a temporal analysis has been performed and the worst dry events have been detected. As a result, considering the 3- and 6-month SPI, several dry periods have occurred during the last century. The oldest events occurred in 1958, with more than 40% of the rain gauges presenting SED, in 1969 (more than 45% of the rain gauges) and in 1973 (more than 40% of the rain gauges). More recently, in this century, the worst drought events have been detected in 2001 and in 2007 with more than 60 and 40% of the rain gauges showing SED, respectively. The 12- and 24-month SPI evidenced a different behaviour when compared to the 3- and 6-month SPI. In particular, the most important drought events occurred after 1970; among these two of the most severe and prolonged drought events have been detected between 1982 and 1984 with 13 and 18 consecutive months with more than 40 and 45% of the rain gauges, presenting SED for the 12-month and the 24-month SPI, respectively. Remarkable events have been also observed in 1973 and 1989 with more than 60% (12-month SPI) and almost 40% (24-month SPI) of the rain gauges presenting SED respectively.

Subsequently, the spatial distribution of the percentage of data falling within the different level of drought has been presented. As a result, for the 3- and 6-month SPI only few areas of New Zealand showed high percentage of drought data, while the 12- and 24-month SPI evidenced wide areas affected by drought mainly located in the central-east side of both Islands.

In addition, a trend analysis has been conducted at seasonal scale (February/Summer, May/Autumn, August/Winter and November/Spring SPI-3), considering the wet and the dry seasons (February and August SPI-6) and at annual scale (December SPI-12 and SPI-24 series). At seasonal scale, a negative trend of the SPI values in summer and autumn and a positive trend in winter and spring have been detected. In particular, as to what concerns the summer period, the negative trend mainly involved the Canterbury, and the Nelson–Marlborough regions. Considering the 6-month SPI, in the dry season, similar percentage values of positive and negative trends have been evaluated, while in the wet season, a predominant negative trend can be observed. The negative trends detected in the dry season are located in the Canterbury region, in the South Island, in the East Cape and Bay of Plenty regions and in the North Island, while the positive trends have been

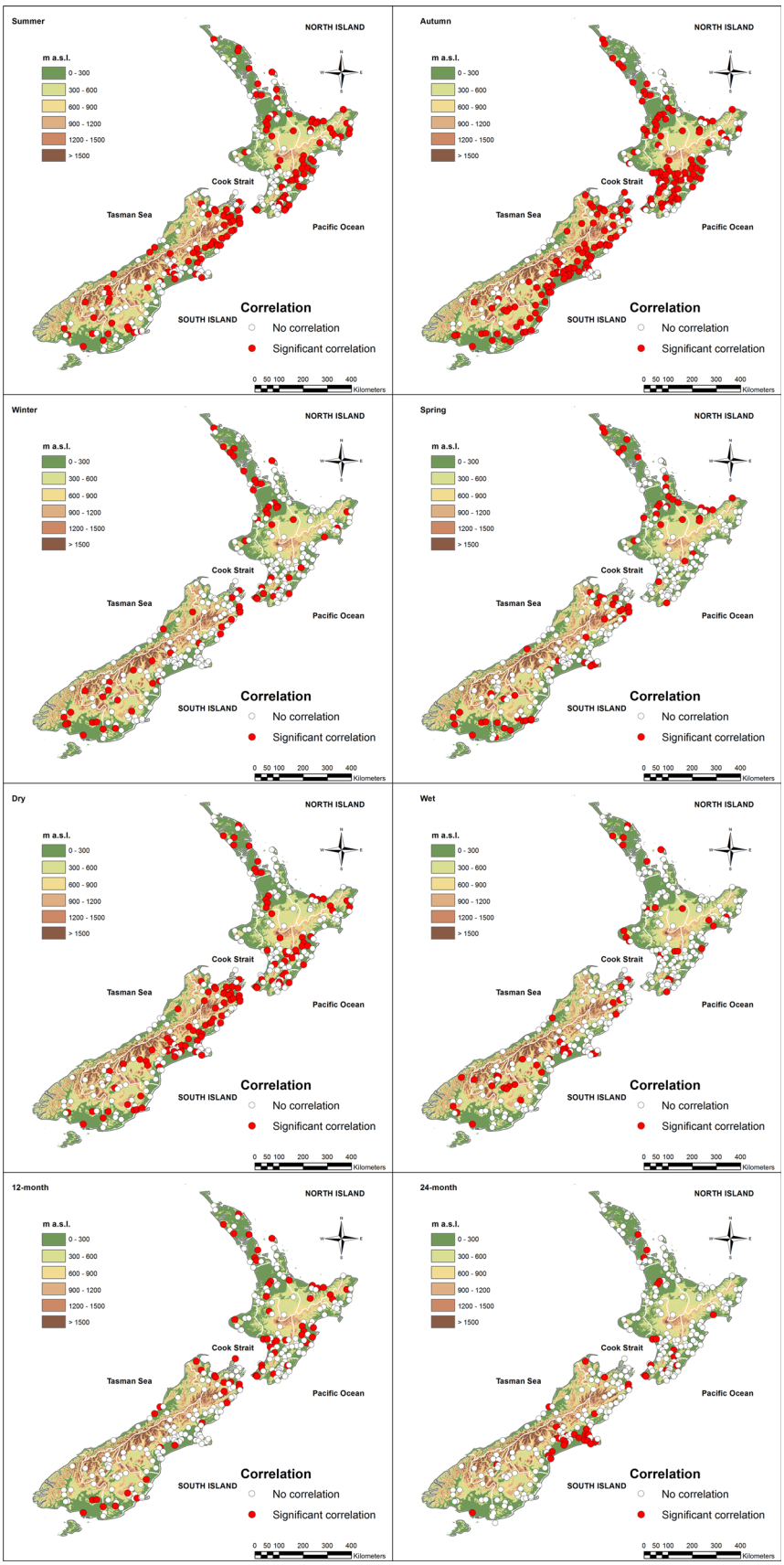

Fig. 7 Correlation between SPI and El Niño values. For each rain gauge, the significance of the correlation coefficient is evidenced through a *different colour*

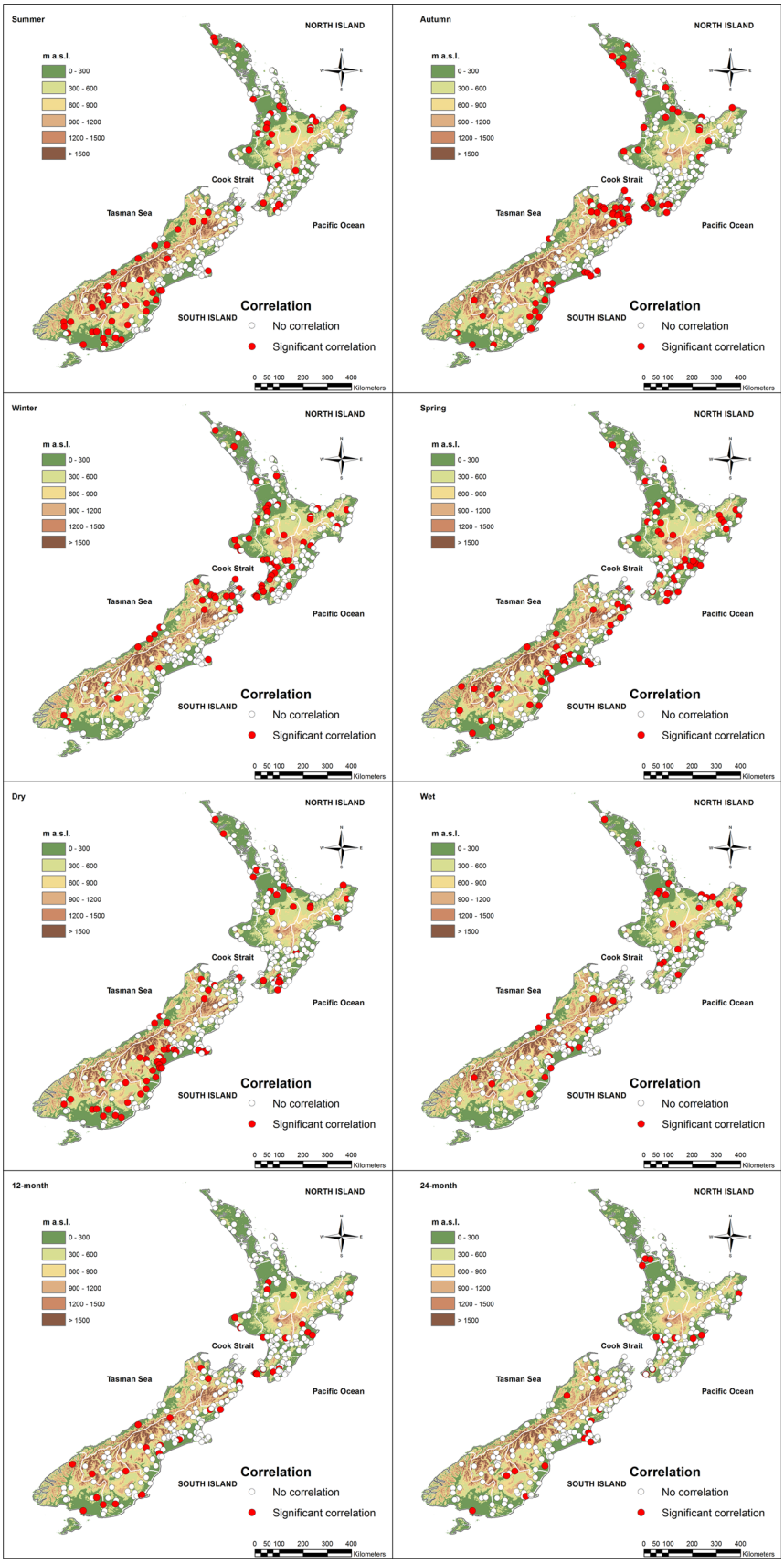

Fig. 8 Correlation between SPI and La Niña values. For each rain gauge, the significance of the correlation coefficient is evidenced through a *different colour*

mainly identified in the Otago, Southland and Nelson–Marlborough regions and in the south-western side of the North Island. At annual scale, a prevalent negative trend can be observed for both the 12-month and the 24-month SPI especially in the Canterbury region and in the eastern side of the Nelson–Marlborough region, in the South Island, and in the Wanganui-Manawatu, East Cape, Hawke's Bay and Bay of Plenty regions, in the North Island.

Finally, the drought response to the global circulation variability has been evaluated through a correlation analysis between drought and the SOI phases. As a result, a clear link existing between drought and the two phases of the climatic index has been evidenced, with El Niño impacting on drought in particular during summer, autumn and in the dry season, in the eastern side of both the islands and with La Niña influencing drought mainly along the coastal areas.

Since drought episodes can severely impact on water resources and their uses, the findings presented in this work, with the identification of the most consistently vulnerable areas, can be useful to plan and manage water supply for household, farming and industrial uses.

Acknowledgements The author would like to thank the National Institute of Water and Atmosphere Research for providing access to the New Zealand meteorological data from the National Climate Database.

References

Abramowitz M, Stegun A (1965) Handbook of mathematical formulas, graphs, and mathematical tables. Dover Publications Inc, New York

Ackerley D, Dean S, Sood A, Mullan AB (2012) Regional climate modeling in NZ: comparison to gridded and satellite observations. Weather Clim 32:3–22

Angelidis P, Maris F, Kotsovinos N, Hrissanthou V (2012) Computation of drought index SPI with alternative distribution functions. Water Resour Manag 26:2453–2473

Bayissa YA, Moges SA, Xuan Y, Van Andel SJ, Maskey S, Solomatine DP, Griensven A, Van Tadesse T (2015) Spatio-temporal assessment of meteorological drought under the influence of varying record length: the case of Upper Blue Nile Basin, Ethiopia. Hydrol Sci J 60:1927–1942

Bonaccorso B, Bordi I, Cancelliere A, Rossi G, Sutera A (2003) Spatial variability of drought: an analysis of the SPI in Sicily. Water Resour Manag 17:273–296

Bordi I, Fraedrich K, Sutera A (2009) Observed drought and wetness trends in Europe: an update. Hydrol Earth Syst Sci 13:1519–1530

Buttafuoco G, Caloiero T (2014) Drought events at different timescales in southern Italy (Calabria). J Maps 10:529–537

Buttafuoco G, Caloiero T, Coscarelli R (2015) Analyses of drought events in Calabria (southern Italy) using standardized precipitation index. Water Resour Manag 29:557–573

Caloiero T (2014) Analysis of daily rainfall concentration in New Zealand. Nat Hazards 72:389–404

Caloiero T (2017) Trend of monthly temperature and daily extreme temperature during 1951–2012 in New Zealand. Theor Appl Climatol 129:111–127

Caloiero T, Sirangelo B, Coscarelli R, Ferrari E (2016) An analysis of the occurrence probabilities of wet and dry periods through a stochastic monthly rainfall model. Water 8:39

Capra A, Scicolone B (2012) Spatiotemporal variability of drought on a short–medium time scale in the Calabria region (Southern Italy). Theor Appl Climatol 3:471–488

Clark A, Mullan A, Porteous A (2011) Scenarios of regional drought under climate change. NIWA Client Report WLG2012-32. National Institute of Water and Atmospheric Research, Wellington

Dravitzki S, McGregor J (2011) Extreme precipitation of the Waikato region, New Zealand. Int J Climatol 31:1803–1812

Edwards D, McKee T (1997) Characteristics of 20th century drought in the United States at multiple scale. Atmos Sci Pap 634:1–30

Estrela T, Vargas E (2012) Drought management plans in the European Union. Water Resour Manag 26:1537–1553

Fang K, Gou X, Chen F, Davi N, Liu C (2013) Spatiotemporal drought variability for central and eastern Asia over the past seven centuries derived from tree-ring based reconstructions. Quat Int 283:107–116

Feng S, Hu Q, Oglesby RJ (2011) Influence of Atlantic sea surface temperatures on persistent drought in North America. Clim Dyn 37:569–586

Garnier B (1950) New Zealand weather and climate. Whitcombe and Tombs Ltd, Christchurch

Griffiths G (2007) Changes in New Zealand daily rainfall extremes 1930–2004. Weather Clim 27:3–44

Griffiths GM (2011) Drivers of extreme daily rainfall in New Zealand. Weather Clim 31:24–49

Griffiths GM, Salinger MJ, Leleu I (2003) Trends in extreme daily rainfall across the South Pacific and relationship to the South Pacific convergence zone. Int J Climatol 23:847–869

Hannaford J, Lloyd-Hughes B, Keef C, Parry S, Prudhomme C (2011) Examining the large-scale spatial coherence of European drought using regional indicators of precipitation and streamflow deficit. Hydrol Process 25:1146–1162

Hua T, Wang XM, Zhang CX, Lang LL (2013) Temporal and spatial variations in the palmer drought severity index over the past four centuries in arid, semiarid, and semihumid East Asia. Chin Sci Bull 58:4143–4152

Huang J, Liu F, Xue Y, Sun SL (2015) The spatial and temporal analysis of precipitation concentration and dry spell in Qinghai, Northwest China. Stoch Environ Res Risk 29:1403–1411

IPCC (2013) Summary for policymakers. Fifth assessment report of the intergovernmental panel on climate change. Cambridge University Press, Cambridge and New York

Jiang N, Griffiths G, Lorrey A (2013) Influence of large-scale climate modes on daily synoptic weather types over New Zealand. Int J Climatol 33:499–519

Kamber G, McDonald C, Price G (2013) Drying out: Investigating the economic effects of drought in New Zealand. Reserve Bank of New Zealand, Wellington

Kendall MG (1962) Rank correlation methods. Hafner Publishing Company, New York

MAF (2009) Regional and national impacts of the 2007–2008 drought. Butcher Partners Ltd, Tai Tapu

Mann HB (1945) Nonparametric tests against trend. Econometrica 13:245–259

McKee TB, Doesken NJ, Kleist J (1993) The relationship of drought frequency and duration to time scale. In: preprints eighth conference on applied climatology, Anaheim, The American Meteor Society, pp 179–184

McKee TB, Doesken NJ, Kleist J (1995) Drought monitoring with multiple time scales. In: Preprints ninth conference on applied climatology, Dallas, The American Meteor Society, pp 233–236

Minetti JL, Vargas WM, Poblete AG, de la Zerda LR, Acuña LR (2010) Regional droughts in southern South America. Theor Appl Climatol 102:403–415

Mullan B, Porteous A, Wratt D, Hollis M (2005) Changes in drought risk with climate change. https://www.beehive.govt.nz/sites/all/files/Drought_Report_Final.pdf. Accessed 26 May 2017

NIWA (2013) Overview of New Zealand Climate. http://www.niwa.co.nz/education-and-training/schools/resources/climate/overview. Accessed 26 May 2017

Oliver JE (2005) Encyclopedia of world climatology. Springer, Netherlands

Palmer JG, Cook ER, Turney CSM, Allen K, Fenwick P, Cook B, O'Donnell AJ, Lough JM, Grierson PFG, Baker P (2015) Drought variability in the eastern Australia and New Zealand summer drought atlas (ANZDA, CE 1500–2012) modulated by the interdecadal Pacific oscillation. Environ Res Lett 10:124002

Salinger MJ, Mullan AB (1999) New Zealand climate: temperature and precipitation variations and their links with atmospheric circulation 1930–1994. Int J Climatol 19:1049–1071

Salinger M, Basher R, Fitzharris B, Hay J, Jones P, Macveigh J, Schmidely-Leleu I (1995) Climate trends in the South-West Pacific. Int J Climatol 15:285–302

Sinclair MR (1994) An objective cyclone climatology for the Southern Hemisphere. Mon Weather Rev 122:2239–2256

Sinclair MR (1995a) A climatology of cyclogenesis for the Southern Hemisphere. Mon Weather Rev 123:1601–1619

Sinclair MR (1995b) An extended climatology of extratropical cyclones over the Southern Hemisphere. Weather Climate 15:21–32

Sirangelo B, Caloiero T, Coscarelli R, Ferrari E (2015) A stochastic model for the analysis of the temporal change of dry spells. Stoch Environ Res Risk 29:143–155

Sirangelo B, Caloiero T, Coscarelli R, Ferrari E (2017) Stochastic analysis of long dry spells in Calabria (Southern Italy). Theor Appl Climatol 127:711–724

Tabari H, Abghari H, Hosseinzadeh Talaee P (2012) Temporal trends and spatial characteristics of drought and rainfall in arid and semi-arid regions of Iran. Hydrol Process 26:3351–3361

Thom HCS (1958) A note on the gamma distribution. Mon Weather Rev 86:117–122

Tomlinson AI (1976) Climate. In: Ward I (ed) New Zealand atlas. Government Printer, Wellington, pp 82–89

Trenberth KE (1991) Storm tracks in the Southern Hemisphere. J Atmos Sci 48:2159–2178

Tsakiris G, Pangalou D, Vangelis H (2007) Regional drought assessment based on the reconnaissance drought index (RDI). Water Resour Manag 21:821–833

Vicente-Serrano SM (2005) El Niño and La Niña influence on droughts at different timescales in the Iberian Peninsula. Water Resour Res 41:W12415

Vicente-Serrano SM (2006) Differences in spatial patterns of drought on different time sales. An analysis of the Iberian Peninsula. Water Resour Manag 20:37–60

Wang G (2005) Agricultural drought in a future climate: results from 15 global climate models participating in the IPCC 4th assessment. Clim Dyn 25:739–753

Wilhite DA, Hayes MJ, Svodoba MD (2000) Drought monitoring and assessment in the U.S. In: Voght JV, Somma F (eds) Drought and drought mitigation in Europe. Kluwers, Dordrecht

Wu H, Hayes MJ, Wilhite DA, Svoboda MD (2005) The effect in the length of record in the standardized precipitation index calculation. Int J Climatol 25:505–520